

1  
2  
3  
4  
5  
6  
7

# Beyond the Virtual Intracranial Stenting Challenge 2007: non-Newtonian and flow pulsatility effects

4 Marco Cavazzuti<sup>a</sup>, Mark Atherton<sup>\*,b</sup>, Michael Collins<sup>b</sup>, Giovanni Barozzi<sup>a</sup>

5 <sup>a</sup>*Dipartimento di Ingegneria Meccanica e Civile, Università degli Studi*  
6 *di Modena e Reggio Emilia, via Vignolese 905, 41125 Modena, Italy*

7 <sup>b</sup>*School of Engineering and Design, Brunel University, West London, UB8 3PH, UK*

---

8 **Abstract**

9 The Virtual Intracranial Stenting Challenge 2007 (visc'07) is becoming a  
10 standard test case in computational minimally-invasive cerebrovascular in-  
11 tervention. Following views expressed in the literature and consistent with  
12 the recommendations of a report, the effects of non-Newtonian viscosity and  
13 pulsatile flow are reported. Three models of stented cerebral aneurysms,  
14 originating from visc'07 are meshed and the flow characteristics simulated  
15 using commercial Computational Fluid Dynamics (CFD) software. We con-  
16 clude that non-Newtonian and pulsatile effects are important to include in  
17 order to discriminate more effectively between stent designs.

18 *Key words:* cerebral aneurysm, visc'07, stent

---

19 **1. Introduction**

20 The work presented here uses benchmark models from the Virtual In-  
21 tracranial Stenting Challenge (VISC 2007), an international initiative to as-  
22 sess the effectiveness of state-of-the-art numerical modelling of blood flow in  
23 stented cerebral aneurysms. The results submitted to visc'07 by six simu-  
24 lation teams (Radaelli *et al.* 2008) highlight the desirability of considering  
25 the effects of *non-Newtonian viscosity* and *flow pulsatility* in future work for  
26 purposes of clinical relevance, both of which were included in our studies  
27 briefly reported here.

---

\*corresponding author

*Email addresses:* mark.atherton@brunel.ac.uk (Mark Atherton), +44(0)1895  
274000 (Mark Atherton)

*Preprint submitted to Elsevier*

*May 4, 2010*

## 28 **2. Methods**

29 The Fluent code was used for the simulations. The following boundary  
30 conditions were set: uniform velocity with  $2.36 \frac{\text{g}}{\text{s}}$  mass flow rate at the inlet,  
31 zero gauge pressure on the outlet and no slip walls, as set by VISC'07.

32 A steady-state laminar solver was used with second order upwind momen-  
33 tum discretization and SIMPLE pressure-velocity coupling. The fluid flowing  
34 in the artery was initially defined as water (as requested by VISC'07), and  
35 later it was changed to blood with density ( $\rho$ )  $1060 \frac{\text{kg}}{\text{m}^3}$  and viscosity ( $\mu$ ) 4 cP.

36 Since a Newtonian model is prone to underestimate the WSS in a CFD  
37 analysis at lower velocity gradients (Chen *et al.* 2006, Lee and Steinman  
38 2006, Gijzen *et al.* 1999a,b), it was decided to investigate a non-Newtonian  
39 formulation as well. The Fluent power-law option for dynamic viscosity (Flu-  
40 ent 2006) was used, as no one model is universally accepted and this is a valid  
41 option at lower shear rates (Johnson *et al.* 2004, Shibeshi and Collins 2005):

$$\mu_{min} < \mu = k \cdot \dot{\gamma}^{n-1} < \mu_{max} \quad (1)$$

42 where  $\mu$  is the dynamic viscosity in  $\frac{\text{kg}}{\text{m s}}$ ,  $k$  is the consistency index whose  
43 value is  $0.0161 \frac{\text{kg s}^{n-2}}{\text{m}}$ ,  $n$  the power-law index is 0.63, and  $\dot{\gamma}$  is the shear rate  
44 in  $\text{s}^{-1}$  (Owen *et al.* 2005).  $\mu_{min}$  and  $\mu_{max}$  are lower and upper limits of the  
45 power-law function and were set to  $10^{-5} \frac{\text{kg}}{\text{m s}}$  and  $1 \frac{\text{kg}}{\text{m s}}$  respectively.

46 In order to address the inclusion of pulsatility (c.f. Radaelli *et al.* 2008  
47 and others), unsteady simulations were configured for the unstented and the  
48 three stented cases. The inlet waveform for a basilar artery (Ford *et al.* 2008)  
49 was slightly modified as follows: the mean flow rate was set to the steady-  
50 state value of  $2.36 \frac{\text{g}}{\text{s}}$  as specified by VISC'07 and implemented in Fluent as  
51 a uniform velocity profile of  $0.179 \frac{\text{m}}{\text{s}}$ ; the pulse rate was set to 70 beats  
52 per minute; and the waveform was slightly smoothed in order to reduce the  
53 number of time steps needed to represent the whole cycle.

54 A standard grid independency procedure on the stented aneurysm models  
55 was carried out, and a suitable meshing of 2.30 million elements meshes was  
56 selected.

## 57 **3. Results**

58 For brevity, we focus the results on two regions of interest. (i) The  
59 aneurysm Neck Section, which corresponds to the minimum section area  
60 of the aneurysm and is comparable with that of cut-plane P2 in Radaelli

61 *et al.* 2008. (ii) Segment x, the first  $\frac{1}{3}$  aneurysm volume immediately after  
 62 the Neck Section. Results are given in terms of mass flow rate and average  
 63 Wall Shear Stress (wss).

64 *3.1. Newtonian vs. non-Newtonian*

65 Referring to the table of results for steady-state (Table 1), the non-  
 66 Newtonian case significantly increases dynamic viscosity and slightly modifies  
 67 mass flow rate in the lower aneurysm area resulting in a much higher average  
 68 WSS. The Newtonian models overestimate mass flow rate by about 3% for  
 69 Stent 1 and Stent 2 and underestimate by just under 2% for Stent 3, whereas  
 70 the average WSS in the Newtonian models is consistently underestimated by  
 71 15-20%.

Table 1: *Comparison between unstented and stented cases for steady-state flow. Percentages refer to difference between stented case and unstented artery.*

Case	Mass Flow (g/s) through Neck Section	Average Dynamic Viscosity (cP = mPa s) in Segment x	Average WSS (Pa) in Segment x
Unstented artery non-Newtonian	0.3809	7.142	2.057
Stent 1 Newtonian	0.3391 -11.0 %	4.000 -44.0 %	1.091 -46.9 %
Stent 2 Newtonian	0.3427 -10.0 %	4.000 -44.0 %	1.054 -48.8 %
Stent 3 Newtonian	0.2738 -28.1 %	4.000 -44.0 %	0.960 -53.3%
Stent 1 non-Newtonian	0.3268 -14.2 %	8.003 +12.1 %	1.296 -37.0 %
Stent 2 non-Newtonian	0.3320 -12.8 %	7.938 +11.1 %	1.282 -37.6 %
Stent 3 non-Newtonian	0.2785 -26.9 %	8.555 +19.8 %	1.195 -41.9 %

72 The results do not contradict Gijzen *et al.* (1999a,b), who, using both ex-  
 73 periments and simulations, essentially state the importance of non-Newtonian  
 74 (shear-thinning) blood modelling since it alters significantly the velocity pro-  
 75 files. As a non-Newtonian model produces higher fluid viscosities in the  
 76 aneurysm region (where the shear rate is low) compared to the Newtonian

77 model, this implies that the fluid tends to reduce its speed much more quickly  
 78 inside the aneurysm, and hence the non-Newtonian model produces a smaller  
 79 mass flow rate. Also, the lower velocity gradient promotes a lower WSS while  
 80 a higher viscosity promotes a higher WSS.

81 In the lower aneurysm, the effect of the increased viscosity is domi-  
 82 nant and the Newtonian model significantly underestimates the average WSS.  
 83 Overall, it seems that the non-Newtonian hypothesis redistributes the veloc-  
 84 ity profiles and the WSS in a more uniform and smooth way and thus peaks  
 85 are smoothed out (Figure 1).

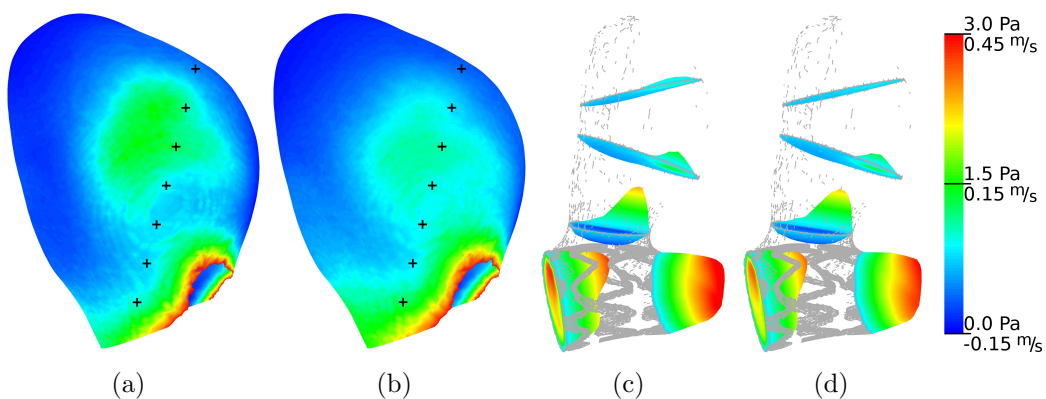


Figure 1: WSS and velocity profiles in aneurysm region for stent 3 steady simulation: Newtonian versus non-Newtonian: (a) WSS, Newtonian case; (b) WSS, non-Newtonian case; (c) velocity profiles, Newtonian case; (d) velocity profiles, non-Newtonian case

### 86 3.2. Pulsatile flow

87 In Figure 2 the mass flow rate entering the aneurysm (i.e. crossing the  
 88 Neck Section) is shown. The pulse cycle in the main artery is also shown  
 89 scaled to  $\frac{1}{5}$ -th of its amplitude.

90 The mass flow rate entering the aneurysm in the unstented case at time  
 91 0 s is equal to  $0.3488 \frac{\text{g}}{\text{s}}$  (15 % of the mass flow rate in the main artery). This  
 92 ratio remains in the range from 10 % to 20 % for all the cases investigated  
 93 and for most of the pulse cycle, except when the mass flow rate in the artery  
 94 drops to its minimum.

95 The presence of the stent reduces the mass flow rate in the aneurysm  
 96 region and also promotes small changes in the phase between the mass flow  
 97 rate in the main artery and in the aneurysm. In fact, the main pulse cycle is

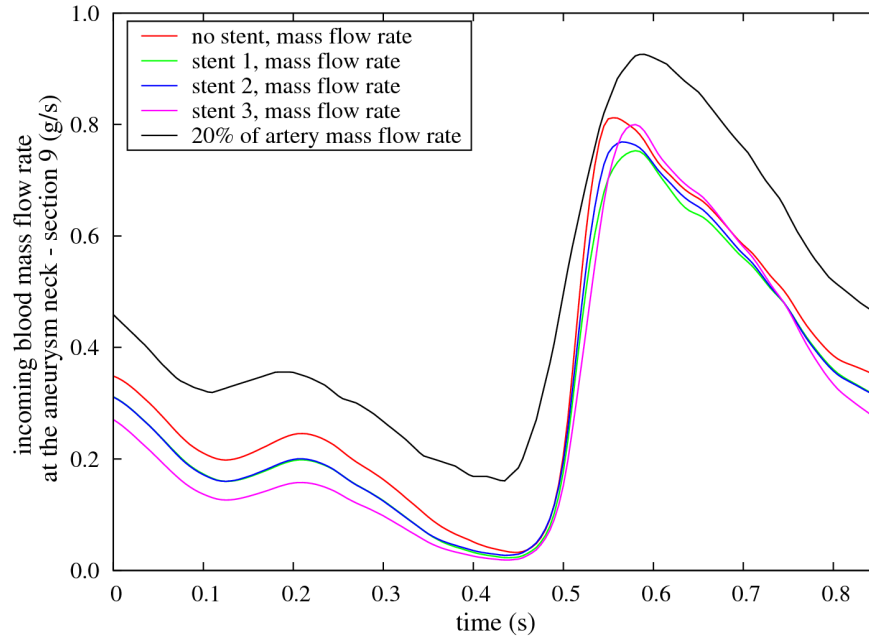


Figure 2: *Mass flow through Section 9*

98 reflected in the aneurysm mass flow rate with a minimum phase delay from  
 99 0 to 0.5s. However, the maximum peak in the aneurysm mass flow rate,  
 100 which is found at  $\approx 0.57$ s for each of the four simulations, anticipates the  
 101 corresponding peak in the main artery, which is found at 0.59s. The change  
 102 in the phase shift, even if small, together with the change in mass flow ratio  
 103 along the cycle suggest the relevance of adopting unsteady simulations for  
 104 better accuracy.

105 The third stent is particularly efficient in reducing the mass flow rate  
 106 entering the aneurysm, in particular in the first half of the pulse cycle with  
 107 reductions ranging from 20% to 50% when compared to the unstented artery.  
 108 The third stent also shows better performance, when compared with the other  
 109 two stents, for more than 75% of the pulse cycle.

### 110 3.3. *Evaluating three stents from VISC'07*

111 Considering the non-Newtonian blood model (see Table 1), the mass flow  
 112 rates of stent 1 and stent 2 are not so different from each other. Stent 2 has  
 113 a higher mass flow rate through the Neck Section ( $0.3320 \frac{g}{s}$  equal to a 12.8%  
 114 reduction in the mass flow rate compared to the unstented case). Stent 3

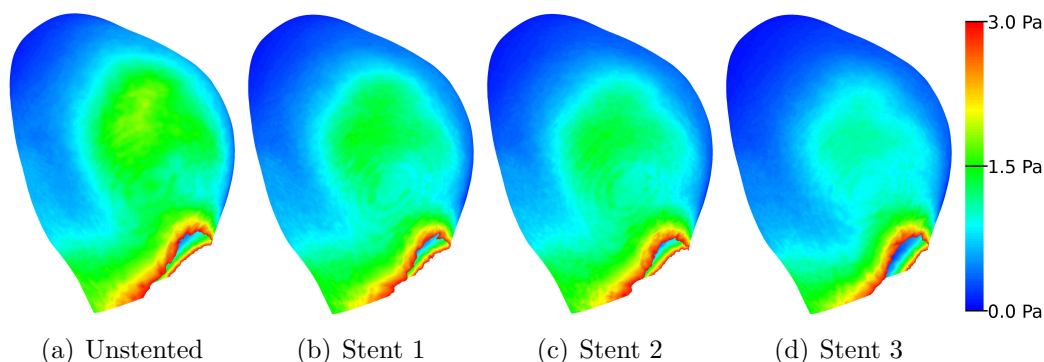


Figure 3: wss on surface of aneurysm for steady non-Newtonian simulations

115 appears to be much more effective in reducing the mass flow rate in the  
 116 aneurysm since the blood crossing the Neck Section in this case amounts to  
 117  $0.2785 \frac{g}{s}$  (a 26.9 % reduction).

118 From these initial considerations stent 3 is expected to be a better clinical  
 119 performer than the other two.

120 Comparing the wss in the unstented case with the three stented models  
 121 (Figure 3 and Table 1), the use of a stent appears to be very effective in  
 122 reducing the wss.

#### 123 4. Conclusions

124 The inclusion of non-Newtonian and pulsatile effects in the visc'07 mod-  
 125 els are shown to be important. Stent 3 emerges as the best design, which is  
 126 consistent with the results published in the literature.

#### 127 Conflict of interest statement

128 The authors have no financial or personal relationships with other people  
 129 or organisations that could inappropriately influence (bias) their work.

#### 130 Acknowledgements

131 We thank Dr Matthieu De Beule from the Institute Biomedical Technol-  
 132 ogy, Ghent University, Belgium for his generous advice on how to implement  
 133 the Magics software. Also, our thanks to Dr Peter Flynn, Consultant Radi-  
 134 ologist, Victoria Hospital, Belfast Trust, for his helpful comments on clinical  
 135 aspects of the paper.

136 **References**

- 137 Chen, J., Lu, X-Y., Wang, W., 2006, Non-Newtonian effects of blood flow  
138 on hemodynamics in distal vascular graft anastomoses. *J. Biomech.* 39  
139 (11), 1983–1995.
- 140 Fluent 6.3 User Guide, 2006, section 8.4.5.
- 141 Ford, M.D., Niklov, H.N., Milner, J.S., Lownie, S.P., DeMont, E.M., Kalata,  
142 W., Loth, F., Holdsworth, D.W., Steinman, D.A., 2008. PIV-measured  
143 versus CFD-predicted flow dynamics in anatomically realistic cerebral  
144 aneurysm models. *J. Biomech. Eng.* 130 (2), 021015 (9 pages).
- 145 Gijsen, F.J.H., van de Vosse, F.N., Janssen, J.D., 1999a. The influence of the  
146 non-Newtonian properties of blood on the flow in larger arteries: steady  
147 flow in a carotid bifurcation model. *J. Biomech.* 32 (6), 601–608.
- 148 Gijsen, F.J.H., Allanic, E., van de Vosse, F.N., Janssen, J.D., 1999b. The  
149 influence of the non-Newtonian properties of blood on the flow in larger  
150 arteries: unsteady flow in a 90° curved tube. *J. Biomech.* 32 (6), 705–  
151 713.
- 152 Johnson, B.M., Johnson, P.R., Corney, S., Kilpatrick, D., 2004. Non-  
153 Newtonian blood flow in human right coronary arteries: steady state  
154 simulations. *J. Biomech.* 37 (5), 709–713.
- 155 Lee, S.-W., Steinman, D.A., 2006. On the relative importance of rheology  
156 for image-based CFD models of the carotid bifurcation. *J. Biomech.* 39  
157 (1), S283.
- 158 Owen, I., Gray, J., Escudier, M., Poole, R., 2005. The importance of the non-  
159 Newtonian characteristics of blood in flow modelling studies. Abstracts  
160 of Second Physiological Flow Network meeting, University of Edinburgh,  
161 26-27 September 2005.
- 162 Radaelli, A.G., Augsburger, L., Cebal, J.R., Ohta, M., Rufenacht, D.A.,  
163 Balossino, R., Benndorf, G., Hose, D.R., Marzo, A., Metcalfe, R.,  
164 Mortier, P., Mut, F., Raymond, P., Soggi, L., Verheghe, B., Frangi,  
165 A.F., 2008. Reproducibility of haemodynamical simulations in a subject-  
166 specific stented aneurysm model – A report on the Virtual Intracranial  
167 Stenting Challenge 2007. *J. Biomech.* 41 (10), 2069–2081.

- 168 Shibeshi, S.S., Collins, W.E., 2005. The Rheology of Blood Flow in a  
169 Branched Arterial System. *Applied Rheology* 15 (6), 398–405.
- 170 VISC 2007 The 1st Virtual Intracranial Stenting Challenge  
171 <http://www.cilab.upf.edu/visc06> (accessed 29 January 2009)